ORIGINAL PAPER

Liquid crystals as additives in solid polymer electrolytes for lithium metal batteries

Isaac Álvarez Moisés[1] · Alessandro Innocenti[2,3] · Mathilde Somville[1] · Benoît Notredame[1] · Stefano Passerini[2,3,4] · Jean-François Gohy[1]

Abstract

The forefront of research for new electrolyte materials for tomorrow's electrochemical energy storage technologies is based on thoroughly designed molecular architectures. Here, liquid crystals (LCs) mixed with poly(ethylene-oxide) (PEO) and lithium salts are proposed as solid polymer electrolytes (SPEs) for application in lithium-metal batteries. The PEO matrix comprises the LC, which gives orientational properties, whereas the PEO chains with lithium salts are responsible for the ionic conductivity. N-(4-Methoxybenzylidene)-4-butylaniline (MBBA) is used as proof-of-concept and new LC molecules are developed for further research. Ionic conductivities ($7 \cdot 10^{-4}$ S·cm^{-1} at 40 °C) up to three times higher than the reference without LC are achieved. In addition, the SPEs are characterized electrochemically, thermally and by polarized optical microscope demonstrating the preservation of the liquid crystalline behavior even after mixing with PEO and lithium salts.

Introduction

Significant effort has been dedicated to develop solid polymer materials for ion transport towards the application in energy related technologies such as lithium batteries, fuel cells and solar cells [1, 2]. Solid organic materials present advantages such as easy processability and film forming properties, which allow their industrialization in large-scale application [3]. Furthermore, the replacement of liquid for solid electrolyte reduces the risk associated with leakage and self-ignition and diminishes dendrite formation, which extends the battery life and reduces the occurrence of short circuits [4, 5].

The most studied solid polymer electrolytes (SPEs) for batteries are based on poly(ethylene oxide) (PEO) and have been firstly reported by Wright [6]. This system presents many advantages over other type of materials, such as good electrochemical stability, excellent compatibility with inorganic salts, low fabrication cost and good safety. However, due to the semi-crystalline behavior, PEO films present low ionic conductivity limiting their application as solid polymer electrolytes for high performance lithium metal batteries (LMB), and being able to operate only at temperatures higher than the melting point of crystallites (60 °C) in commercial setups [7]. However, relevant key points can be addressed for their widespread use. Firstly, the ionic conductivity of PEO ($\sigma \approx 10^{-6}$ S·cm^{-1} at 25 °C) is several orders of magnitude lower than common liquid electrolytes ($\sigma \approx 10^{-2}$ S·cm^{-1} at 25 °C). Secondly, polymer electrolytes are usually characterized by a low lithium transference number ($t_{Li}^+ < 0.3$) which consequently leads to polarization phenomena limiting the power density of the battery device [8].

The addition of liquid plasticizers, ionic liquids or inorganic particles has been proved to be a reliable strategy for increasing the ionic conductivity and decreasing the polarization effects [9]. Furthermore, liquid crystals (LC) have attracted much attention as organic-based electrolytes for ion-transport materials because of their natural anisotropic molecular self-arrangement [10–14]. LC are materials combining anisotropy and molecular dynamics, and these properties are of a great use in electrochemical devices. For example, LCs have been employed in electro-optical

✉ Jean-François Gohy
jean-francois.gohy@uclouvain.be

1   Catholic University of Louvain (UCLouvain), Place de l'Université 1, 1348 Louvain-la-Neuve, Belgium

2   Helmholtz Institute Ulm (HIU), 89081 Ulm, Germany

3   Karlsruhe Institute of Technology (KIT), 76021 Karlsruhe, Germany

4   Department of Chemistry, Sapienza University of Rome, P. A. Moro 5, 00185 Rome, Italy

displays. Recently, Kato et al. have reported LCs with lithium ionic conductivity [11, 15].

Here, we intend to prepare a SPE comprising LC domains incorporated in the PEO matrix. The LC is employed as an additive, which is introduced into the SPE formulation aiming to increase the ionic conductivity of PEO by the anisotropy of the mesogenic structures formed inside the PEO matrix, that could further affect the orientation of the PEO chains to create lithium ions conduction pathways. Moreover, the presence of LC domains is expected to reduce the crystallinity of the PEO matrix. Additionally, the stickiness of the LC-containing SPE membrane is expected to improve the contact interlayer between electrodes and SPE.

Results and discussion

Design of solid polymer electrolytes

A new class of SPE was designed based on PEO comprising a low molar mass thermotropic LC as additive for their use in LMB. PEO was selected because it is the most studied polymer electrolyte for LMB and it can be used conveniently as a reference. N-(4-Methoxybenzylidene)-4-butylaniline (MBBA) displays a nematic liquid crystalline state at near-room temperature (25–45 °C) giving the opportunity to exploit its liquid crystal properties in a temperature range of practical interest. The molar ratio between EO:LC:Li was set to 10:0.5:1 because it resulted in homogenous sticky membranes which did not break easily upon elongation (Fig. 1). Accordingly, the sample reference was set to EO:Li 10:1 molar ratio. Additionally, benzophenone was added to all samples (5% weight of PEO) for crosslinking purposes, increasing the mechanical properties.

Fig. 1 Picture of solid polymer electrolyte membrane with LC as additive

Thermal behavior and liquid crystallinity

Figure 2 shows the differential scanning calorimetry (DSC) measurements performed on PEO/MBBA/LiTFSI. For comparison, the DSC traces of PEO/LiTFSI, 0.5 M solution of LiTFSI in MBBA (MBBA/LiTFSI) and MBBA are also shown. For all the samples containing MBBA, liquid crystalline properties are observed as confirmed by the melting point at 24 °C and the isotropic point at 46 °C. This proves that the MBBA molecules gather together to form liquid crystalline domains inside the polymer matrix, which may give a contribution towards the enhancement of the ionic conductivity. The peak appearing around 15 °C for the PEO/MBBA/LiTFSI sample is most likely due to the melting of some excess LiTFSI phase as reported elsewhere [16].

The PEO/LiTFSI sample presents a broad peak at 65 °C due to the melting of the PEO crystalline domains [7], whereas this peak shifts to lower temperature (30 °C) in the PEO/MBBA/LiTFSI sample. The introduction of MBBA reduces the degree of crystallinity of PEO by 95% by the comparison of the enthalpy of these two signals.

The birefringence of the MBBA, MBBA/LiTFSI and PEO/MBBA/LiTFSI samples was studied by polarizing optical microscopy (POM). The microphotographs at 40 °C are shown in Fig. S1 in the supporting information (SI), revealing the liquid crystal nematic texture of MBBA (Fig. S1a), as previously reported [17]. The nematic mesophase is maintained after addition of LiTFSI to MBBA (Fig. S1b), although the observed texture is somewhat different from the one initially observed for pure MBBA, indicating the doping
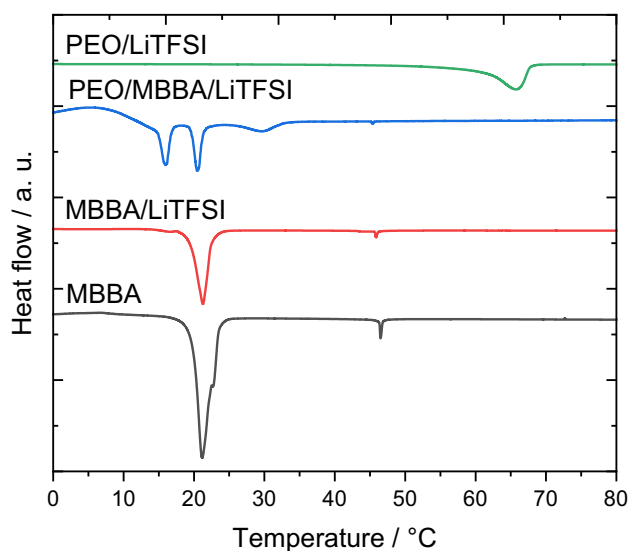

Fig. 2 Differential scanning calorimetry thermograms of PEO/LiTFSI (green), PEO/MBBA/LiTFSI (blue), 0.5 M solution of LiTFSI in MBBA (red) and MBBA (black)

of LC affects their self-orientation. A completely different texture is observed for the PEO/MBBA/LiTFSI SPE (Fig. S1c), showing the homogenous dispersion of the LC in the PEO matrix. Since no crystalline PEO domains are observed in the PEO/MBBA/LiTFSI SPE (Fig. 2), the birefringent features observed in Fig. 1C are exclusively attributed to the LC mesophase and reveal a dense network-like structure with channels that could play the role of ionic conduction pathways for lithium ions. This agrees with the second transition observed by DSC (*i. e.*, the liquid crystal transition to isotropic liquid). In the case of MBBA/LiTFSI and PEO/MBBA/LiTFSI, the isotropization appears at 45 °C (Fig. 2), 45 °C), demonstrating that at 40 °C the liquid crystalline mesophases are still present. Indeed, POM pictures at 50 °C reveal no birefringent features confirming the isotropic state.

Ionic conductivity

The temperature dependence of the ionic conductivity is presented in Fig. 3. The incorporation of a LC into a PEO-based SPE increases its ionic conductivity (σ) whatever the temperature, e.g., from $9 \cdot 10^{-5}$ S cm^{-1} to $2 \cdot 10^{-4}$ S cm.$^{-1}$ at 40 °C. This improvement could result from the incorporation of the LC that, at the same time, suppresses the crystallinity of PEO (Fig. 2) and forms a network-like structure (Fig. S1c) that could provide conduction pathways for lithium ions. Additionally, the stickiness of the LC loaded SPE improves the contact interlayer between electrodes and SPE. Moreover some LC molecules could percolate to the PEO phase and play a plasticizer effect, which increases the free volume between the polymer chains leading to higher chain mobility and better ionic conductivity [18]. Larger loading amounts of LC do not result in higher conductivities
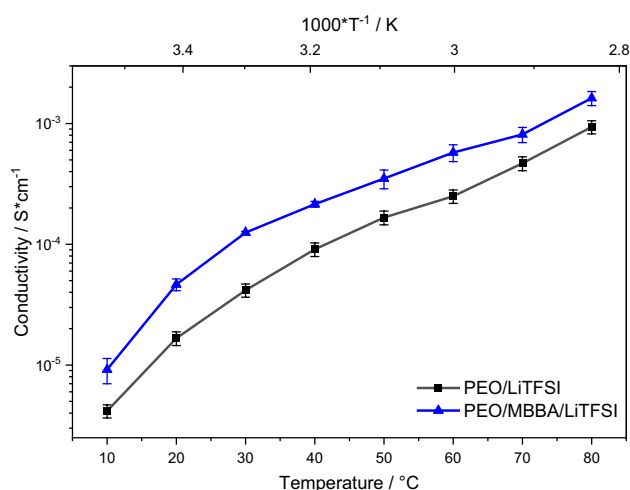
suggesting that the LC itself is not responsible for the ionic conductivity. Although the improvement of the ionic conductivity is observed over the entire range of measured temperatures, there is a slightly higher enhancement at 30 and 40 °C, exactly when MBBA is in its liquid crystalline mesophase, indicating that the self-orientation of the mesogens may be a reason for this improvement. The cross-linking of the sample does not affect the conductivity at moderate or high temperatures, since only at temperatures below zero a slight decrease in conductivity can be noticed as previously discussed by Kim et al. [19].

Electro chemical stability window (ESW)

The electrochemical stability windows (ESW) of the SPEs measured in Li/SPE/Ni cells at 40 °C are depicted in Fig. S2 in the supporting information (SI). A clear difference can be noticed between the PEO/LiTFSI and PEO/MBBA/LiTFSI samples, since PEO/LiTFSI shows a wider ESW. In particular, in the anodic scan, PEO/MBBA/LiTFSI decomposes at a lower voltage, revealing the lower oxidation resistance of MBBA restricting its use for high-voltage cathode materials. This behavior can be associated to the reversible dynamic bond of imines. Nevertheless, SPEs containing imine bonds have exhibited good cycling performances with LiFePO$_4$/Li [20, 21]. Furthermore, new MBBA derivatives targeting higher oxidation resistance were developed with the support of Density Functional Theory as previously reported by Kato et al. [11].

Lithium stripping-plating (LSP)

The cyclability of lithium metal electrodes in PEO/LiTFSI and PEO/MBBA/LiTFSI was evaluated by stripping-plating tests on symmetric Li/SPE/Li cells at 40 °C (Fig. S3 in the SI). The cell overvoltage was recorded during the galvanostatic tests where each electrode performs as source and sink of lithium ions alternatively. PEO/MBBA/LiTFSI performed in a very reversible way up to 1000 stripping-plating cycles (Fig. S3a). Nevertheless, the gain in ionic conductivity happens at the expense of a increase in overvoltage (0.05 V) in stripping and plating. Figure S3b shows the first 10 cycles demonstrating that at the beginning the overpotential of PEO/MBBA/LiTFSI is only slightly higher than of PEO/LiTFSI. Due to the long-lasting experiment, the MBBA decomposes irreversibly (as shown in Fig. S2) passivating some minor lithium surface causing the increase of a constant overpotential.This energy loss might be overcomed with the introduction of a MBBA derivatives with higher oxidation resistance and carrying a lithium-ion solvating group. In addition, an impedance measurement was taken after the completion of 1000 cycles and it does not show any substantial change with respect to that of the reference. Both

Fig. 3 Ionic conductivity of PEO/LiTFSI (black) and PEO/MBBA/LiTFSI (blue) solid polymer electrolytes as a function of the temperature

cells showing similar R_{int} value $275 \pm 80\ \Omega$ within the practicable range (Fig. S4 in the SI). The low frequency associated with the Warburg impedance presents a slope of 45°indicating a smooth lithium surface without major dendritic growth or mossy lithium, which would cause the angle depression.

Design of new MBBA derivative molecules

The approach of using LCs as additive in SPEs is promising, and in this context, MBBA was used as proof-of-concept. Nevertheless, it is evident that MBBA does not contain a conventional lithium-ion solvating group (*e.g.* ether group), which could further improve the SPE properties. Hence, MBBA derivates were developed with the aim of combining the properties of liquid crystals and ionic conduction, as previously reported by Kato et al. where LC with ion-conducting moieties were designed [11, 12]. New LC molecules, namely CBBA and TBBA, were thus synthesized and their structures are shown in Fig. 4 (the synthesis route and procedure are shown in Fig. S4 in the SI) [22, 23]. They were designed taking into consideration conventional liquid electrolytes for lithium-ion batteries, i.e., cyclic carbonate and ethylene oxide moieties were incorporated. The LC properties of CBBA and TBBA were analyzed by POM (Fig. S1 in the SI). Both molecules showed POM textures characteristic of smectic mesophases. In the case of TBBA, the observed texture suggests a homeotropic alignment of the smectic mesophase. Further characterization of their LC properties has to be conducted, as well as the electrochemical characterization of the SPEs formed after their mixing with PEO and lithium salts.

Experimental section

Materials

All solvents were purchased from VWR. 4-Hydroxybenzaldehyde, 4-butylaniline, p-toluenesulfonyl chloride, sodium hydride, tetraethylene glycol and benzophenone were purchased from SigmaAldrich. Triethylamine, potassium carbonate and lithium bis(trifluoromethanesulfonyl) imide were purchased from Fluorochem. Glycerol carbonate was purchased from ABCR. PEO was purchased from Dow Chemical (WSR 301, Mw = 4,000,000). All chemicals were used as received except if specified otherwise.

Sample preparation

The samples were prepared inside a dry room. PEO (50 mg), MBBA dried with molecular sieve (15 mg), LiTFSI (32 mg) with molar ratio of 10:0.5:1 and benzophenone (2.4 mg) were added to a vial (5 ml) and mixed with the spatula until a homogeneous paste. The paste was sealed in vacuum in aluminum-coated plastic film and annealed at 100 °C for 24 h. After, it was taken from the aluminum-coated bag and placed between Mylar-film films to hot press it at 100 °C under 10 bar and then 20 bar for two minutes, respectively, resulting in circular SPE with 120 µm thickness and 10 cm diameter approximately. Immediately after, the SPE was photo-polymerized from both sides for three minutes each in a UV photo polymerization chamber (Cube photo-irradiator, 350 W Hg lamp). All this procedure was performed in a dry room with dew point < −70 °C at 20 °C.

Characterization

DSC & TGA

The thermal behavior of the system was studied using a Q1000 TA Instruments calorimeter with a heating or cooling rate of 5 °C·min⁻¹ and a thermo-gravimetrical analysis equipment Q500 from TA Instruments calibrated with indium with a heating rate of 10 °C·min⁻¹.

POM

Samples were examined in transmission mode with crossed polarizers under 100 × magnification with a microscope Olympus Provis AX70 equipped with a Mettler FP 90 hot stage.

Ionic conductivity measurements

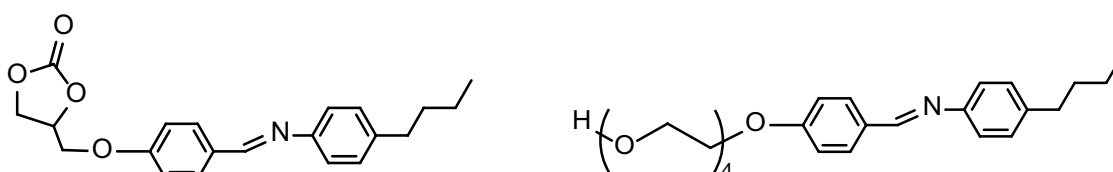Symmetric Cu/Cu pouch cells were used for testing the ionic conductivity inside a climate chamber with temperature

Fig. 4 Structure of MBBA derivatives, 4-butylphenyl)imino)methyl)phenoxy)methyl)-1,3-dioxolan-2-one (CBBA) and 4-butylphenyl)imino) methyl)phenol (TBBA)

control (Binder GmbH) connected to a frequency response analyzer (Solartron 1260A, Ametek) operating in a $0.1–10^6$ Hz frequency range at the amplitude of 10 mV. The conductivity of the polymer films was calculated using the value of electrical resistance obtained by fitting the data to the equivalent circuit model with the Solartron software. Conductivity temperature scans were performed in 10 °C increments at a 0.33 °C·min^{-1} heating rate with an equilibration time of 30 min at each measurement point from 80 to 10 °C. The ionic conductivity was calculated using the following equation:

$$\sigma = \frac{d}{A \cdot R_b}$$

where d is the thickness, A is the area and R_b is the bulk resistance of the SPE film.

Electrochemical stability window & Lithium stripping plating

Measurements were performed at 40 °C inside a climate chamber with temperature control (Binder GmbH) using a multichannel potentiostat (VMP Biologic-Science Instruments). The lithium foil (Honjo) had a thickness of 500 μm.

ESW: Asymmetric cells (Li/SPE/Ni) over the potential range of 0–5 V (vs. Li/Li$^+$) with a scan rate of 0.1 mV·s^{-1}. One cell was used for the anodic scan and another one for the cathodic scan.

Lithium stripping-plating: Symmetric cells (Li/SPE/Li) with a current density of 0.1 mA cm^{-2} where every hour the polarity was reversed.

Conclusions

Liquid crystals were employed as additives for PEO-based solid polymer electrolytes with the aim to increase the overall ionic conductivity via the anisotropy of the mesogenic mesophases formed inside the polymer matrix. An enhancement of the ionic conductivity was demonstrated increasing from $9 \cdot 10^{-5}$ S cm^{-1} to $2 \cdot 10^{-4}$ S cm^{-1} at 40 °C. However, the ESW and LSP experiments showed that the LC additive causes minor increase of overvoltage and reduced ESW. Nevertheless, the results show a promising new approach for the formulation of SPEs increasing the ionic conductivity. Moreover, new MBBA derivates were developed (CBBA and TBBA) with the aim of improving the properties of MBBA, combining the properties of liquid crystals and ionic conduction. Further LC properties characterization as well as electrochemical experiments, including lithium metal full cells, using CBBA and TBBA as LC additive are planned to be conducted.

Declarations

References

1. A. Concellón, T. Liang, A.P.H.J. Schenning et al., Proton-conductive materials formed by coumarin photocrosslinked ionic liquid crystal dendrimers. J. Mater. Chem. C **6**(5), 1000–1007 (2018)
2. T. Kobayashi, T. Ichikawa, T. Kato et al., Development of glassy bicontinuous cubic liquid crystals for solid proton-conductive materials. Adv. Mater. **29**(4), 1604429 (2017)
3. A. Arya, A.L. Sharma, Insights into the use of polyethylene oxide in energy storage/conversion devices: a critical review. J. Phys. D Appl. Phys. **50**(44), 443002 (2017)
4. V. Etacheri, R. Marom, R. Elazari et al., Challenges in the development of advanced Li-ion batteries: a review. Energy Environ. Sci. **4**(9), 3243 (2011)
5. M.M. Kabir, D.E. Demirocak, Degradation mechanisms in Li-ion batteries: a state-of-the-art review. Int. J. Energy Res. **41**(14), 1963–1986 (2017)
6. P.V. Wright, Electrical conductivity in ionic complexes of poly(ethylene oxide). Br. Polym. J. **7**, 319–327 (1975)
7. S. Zhao, Q. Wu, W. Ma et al., Polyethylene oxide-based composites as solid-state polymer electrolytes for lithium metal batteries: a mini review. Front. Chem. **8**, 640 (2020)
8. S. Nurul'Afini Mohd Johari, A review: ionic conductivity of solid polymer electrolyte based polyethylene oxide. Int. J. Electrochem. Sci. (2021). https://doi.org/10.20964/2021.10.53
9. L. Porcarelli, A.S. Shaplov, F. Bella et al., Single-ion conducting polymer electrolytes for lithium metal polymer batteries that operate at ambient temperature. ACS Energy Lett. **1**(4), 678–682 (2016)
10. T. Ohtake, H. Ohno, T. Kato et al., Liquid-crystalline complexes of a lithium salt with twin oligomers containing oxyethylene spacers: an approach to anisotropic ion conduction. Polym. J. **31**(11–2), 1155–1158 (1999)
11. A. Kuwabara, M. Enomoto, E. Hosono et al., Nanostructured liquid-crystalline Li-ion conductors with high oxidation resistance:

molecular design strategy towards safe and high-voltage-operation Li-ion batteries. Chem. Sci. **11**(39), 10631–10637 (2020)

12. K. Kishimoto, Y. Sagara, T. Kato et al., Two dimensionally ion-conductive liquid crystals of cholesterol/tetra(ethylene oxide) block molecules. Mol. Crystals Liquid Crystals **435**(1), 117[777]-125[785] (2005)

13. T. Kato, N. Mizoshita, Self-assembly and phase segregation in functional liquid crystals. Curr. Opin. Solid State Mater. Sci. **6**(6), 579–587 (2002)

14. S. Wang, A. Wang, C. Yang et al., Six-arm star polymer based on discotic liquid crystal as high performance all-solid-state polymer electrolyte for lithium-ion batteries. J. Power Sources **395**, 137–147 (2018)

15. D. Bresser, M. Leclere, L. Bernard et al., Organic liquid crystals as single-ion Li+ conductors. Chemsuschem **14**(2), 655–661 (2021)

16. J. Shin, Ionic liquids to the rescue? Overcoming the ionic conductivity limitations of polymer electrolytes. Electrochem. Commun. **5**(12), 1016–1020 (2003)

17. H. Kelker, B. Scheurle, A liquid-crystalline (nematic) phase with a particularly low solidification point. Angew. Chem. **81**, 902 (1969)

18. F. Cadogan, C. J. Howick, Plasticizers. In *Ullmann's encyclopedia of industrial chemistry*. Wiley-VCH Verlag GmbH & Co KGaA: Weinheim, Germany (2000)

19. G.T. Kim, G.B. Appetecchi, M. Carewska et al., UV cross-linked, lithium-conducting ternary polymer electrolytes containing ionic liquids. J. Power Sources **195**(18), 6130–6137 (2010)

20. X. Cao, P. Zhang, N. Guo et al., Self-healing solid polymer electrolyte based on imine bonds for high safety and stable lithium metal batteries. RSC Adv. **11**(5), 2985–2994 (2021)

21. K. Deng, S. Zhou, Z. Xu et al., A high ion-conducting, self-healing and nonflammable polymer electrolyte with dynamic imine bonds for dendrite-free lithium metal batteries. Chem. Eng. J. **428**, 131224 (2022)

22. A.-C. Simao, B. Lynikaite-Pukleviciene, C. Rousseau et al., 1,2-glycerol carbonate: a versatile renewable synthon. ChemInform (2007). https://doi.org/10.1002/chin.200716116

23. N. Mohr, C. Kappel, S. Kramer et al., Targeting cells of the immune system: mannosylated HPMA-LMA block-copolymer micelles for targeting of dendritic cells. Nanomedicine **11**(20), 2679–2697 (2016)